

Investigations on Power Allocation Among Beams in Non-orthogonal Access with Random Beamforming and Intra-beam SIC for Cellular MIMO Downlink

Yuta Hayashi[†], Yoshihisa Kishiyama[‡], and Kenichi Higuchi^{†(*)}

[†]Graduate School of Science and Technology, Tokyo University of Science

[‡]Radio Access Network Development Department, NTT DOCOMO, INC.

E-mail: ^(*)higuchik@rs.noda.tus.ac.jp

Abstract—We propose an enhancement to the power allocation among multiple beams in our previously reported non-orthogonal access with random beamforming and intra-beam successive interference canceller (SIC) for cellular multiple-input multiple-output (MIMO) downlink. By equally allocating transmission power among multiple beams, the average user throughput within a cell can be enhanced due to the effective use of spatial multiplexing. The throughput of users at the cell edge may be improved by allocating non-equal transmission power among beams since the inter-beam interference is decreased and the received signal power is increased from the viewpoint of the main beam to which most of the transmission power is allocated. Aiming at further enhancement of the system efficiency and cell-edge user experience in our previous non-orthogonal access scheme, we propose coordinated frequency block-dependent inter-beam power allocation and inter-frequency block power allocation based on fractional frequency reuse (FFR) for inter-cell interference coordination. Based on simulation results, we show that the proposed power allocation method effectively enhances the tradeoff between the average and cell-edge user throughput.

I. INTRODUCTION

Orthogonal access based on orthogonal frequency division multiple access (OFDMA) or single carrier-frequency division multiple access (SC-FDMA) is adopted in the 3.9 and 4th generation mobile communication systems such as LTE [1] and LTE-Advanced [2, 3]. Orthogonal access is a reasonable choice for achieving good system-level throughput performance in packet-domain services using channel-aware time- and frequency-domain scheduling with simple single-user detection at the receiver. However, for systems beyond 4G, e.g., LTE-Advanced, further enhancement of the system throughput and cell-edge user experience is required considering the recent exponential increase in the volume of mobile traffic and the need for enhanced delay-sensitive high-volume services such as video streaming and cloud computing. To accommodate such demands, non-orthogonal access can be a promising candidate as a wireless access scheme for systems beyond 4G. To make non-orthogonal access promising, it should be used with advanced transmission/reception techniques such as a successive interference canceller (SIC) [4-7], which is different from the 3rd generation mobile communication systems. We assume that basic transmission signal generation is based on orthogonal frequency division multiplexing (OFDM), including discrete Fourier transform (DFT)-spread OFDM [1], which is robust against multipath interference. The channelization for non-orthogonal user multiplexing within the same frequency is solely obtained through capacity-achieving channel codes such as the turbo code and low-density parity check (LDPC) code. Thus, non-orthogonal user multiplexing forms superposition coding.

Our previous investigations, e.g., [8], showed the potential gain of non-orthogonal access with a SIC in the cellular downlink compared to orthogonal access. We recently proposed a non-orthogonal access scheme with intra-beam superposition coding and SIC for the multiple-input multiple-output (MIMO) downlink [9]. This scheme can achieve a system-level throughput gain compared to the orthogonal access without increasing the overhead of the (orthogonal) reference signals dedicated to the respective users when the number of multiplexed users is increased beyond the number of transmitter antennas due to non-orthogonal user multiplexing. The scheme can work with a SIC at the user terminal receiver instead of dirty paper coding (DPC) at the base station transmitter. The SIC is less complex and more robust against channel variation due to fading than DPC. Furthermore, open loop-based random beamforming [10, 11] is used for beamforming control. Random beamforming is effective in reducing the channel state information feedback.

This paper proposes a method for enhancing the tradeoff between the average and cell-edge user throughput in a non-orthogonal access scheme with random beamforming and an intra-beam SIC. In the proposed method, by equally allocating transmission power among multiple beams, the average user throughput within a cell can be enhanced due to the effective use of spatial multiplexing. On the other hand, the throughput of users at the cell edge may be improved by non-equal transmission power allocation among beams since the inter-beam interference is decreased and the received signal power is increased from the viewpoint of the main beam to which most of the transmission power is allocated.

Meanwhile, the throughput of the users near the cell edge is severely limited by the inter-cell interference in general. A promising approach for mitigating the inter-cell interference problem is employing frequency reuse between neighboring cells. In particular, fractional frequency reuse (FFR), e.g., in [12] and [13], which allows users under different channel conditions to enjoy different reuse factors, achieves a tradeoff between the frequency bandwidth utilization per cell and the impact of inter-cell interference.

From the above observation, we propose a joint transmission power allocation control method among frequency blocks and beams. By effectively combining different power allocations among frequency blocks based on the FFR principle and frequency block-dependent power allocation among multiple beams, the tradeoff between the average and cell-edge user throughput is enhanced. The remainder of the paper is organized as follows. Section II describes our previously reported non-orthogonal access with random beamforming and an intra-beam SIC. Then, Section III

describes the proposed joint transmission power allocation control method. Section IV presents simulation results on the system-level throughput. Finally, Section V concludes the paper.

II. NON-ORTHOGONAL ACCESS WITH RANDOM BEAMFORMING AND INTRA-BEAM SIC

A. Non-orthogonal Access Using Intra-beam Superposition Coding and SIC

We assume OFDM signaling with a cyclic prefix, although we consider non-orthogonal user multiplexing. Therefore, the inter-symbol interference and inter-carrier interference are perfectly eliminated assuming that the length of the cyclic prefix is sufficiently long so that it covers the entire multipath delay spread. There are F frequency blocks and the bandwidth of a frequency block is W Hz. The number of transmitter antennas at the base station is M . The number of receiver antennas at the user terminal is N . For simplicity, in the following, we describe the proposed method at some particular time-frequency block (resource block) f ($f = 1, \dots, F$). For multiple time-frequency blocks, the same process is performed independently in principle. The time index is omitted for simplicity.

The base station performs MIMO transmission with B beams, where $1 \leq B \leq M$. The M -dimensional b -th ($b = 1, \dots, B$) transmitter beamforming vector at frequency block f is denoted as $\mathbf{m}_{f,b}$. We assume that the multiuser scheduler schedules a set of users, $S = \{i(f,b,1), i(f,b,2), \dots, i(f,b,k(f,b))\}$, to beam b of frequency block f . Term $i(f,b,u)$ indicates the u -th ($u = 1, \dots, k(f,b)$) user index scheduled at beam b of frequency block f , and $k(f,b)$ denotes the number of simultaneously scheduled users at beam b of frequency block f . At the base station transmitter, each $i(f,b,u)$ -th user information bit sequence is independently channel coded and modulated. Term $s_{i(f,b,u),f,b}$ denotes the coded modulation symbol of user $i(f,b,u)$ at beam b of frequency block f . We assume $\mathbb{E}[|s_{i(f,b,u),f,b}|^2] = 1$. The allocated transmission power for user $i(f,b,u)$ at beam b of frequency block f is denoted as $P_{i(f,b,u),f,b}$. In the proposed method, $s_{i(f,b,u),f,b}$ of all $k(f,b)$ users is first superposition coded as intra-beam superposition coding and then multiplied by the transmitter beamforming vector, $\mathbf{m}_{f,b}$. Finally, by accumulating all B beam transmission signal vectors, the M -dimensional transmission signal vector, \mathbf{x}_f , at frequency block f is generated as

$$\mathbf{x}_f = \sum_{b=1}^B \mathbf{m}_{f,b} \sum_{u=1}^{k(f,b)} \sqrt{P_{i(f,b,u),f,b}} s_{i(f,b,u),f,b}. \quad (1)$$

The transmission power allocation constraint is represented as

$$\sum_{u=1}^{k(f,b)} P_{i(f,b,u),f,b} = P_{f,b}, \quad \sum_{b=1}^B P_{f,b} = P_f, \quad \sum_{f=1}^F P_f = P_{\text{total}}, \quad (2)$$

where $P_{f,b}$ is the transmission power of beam b at frequency block f , P_f is the total transmission power allocated to frequency block f , and P_{total} is the total transmission power.

The N -dimensional received signal vector of user $i(f,b,u)$ at frequency block f , $\mathbf{y}_{i(f,b,u),f}$, is represented as

$$\begin{aligned} \mathbf{y}_{i(f,b,u),f} &= \mathbf{H}_{i(f,b,u),f} \mathbf{x}_f + \mathbf{w}_{i(f,b,u),f} \\ &= \mathbf{H}_{i(f,b,u),f} \sum_{b=1}^B \mathbf{m}_{f,b} \sum_{u=1}^{k(f,b)} \sqrt{P_{i(f,b,u),f,b}} s_{i(f,b,u),f,b} + \mathbf{w}_{i(f,b,u),f} \end{aligned}, \quad (3)$$

where $\mathbf{H}_{i(f,b,u),f}$ is the $N \times M$ -dimensional channel matrix between the base station and user $i(f,b,u)$ at frequency block f ,

and $\mathbf{w}_{i(f,b,u),f}$ denotes the receiver noise plus inter-cell interference vector at frequency block f .

In the proposed method, the user terminal first performs spatial filtering to suppress the inter-beam interference. Assuming that user $i(f,b,u)$ uses the N -dimensional spatial filtering vector, $\mathbf{v}_{i(f,b,u),f,b}$, to receive beam b of frequency block f , the scalar signal after the spatial filtering, $z_{i(f,b,u),f,b}$, is represented as

$$\begin{aligned} z_{i(f,b,u),f,b} &= \mathbf{v}_{i(f,b,u),f,b}^H \mathbf{y}_{i(f,b,u),f} \\ &= \mathbf{v}_{i(f,b,u),f,b}^H \mathbf{H}_{i(f,b,u),f} \mathbf{m}_{f,b} \sum_{u'=1}^{k(f,b)} \sqrt{P_{i(f,b,u'),f,b}} s_{i(f,b,u'),f,b} \\ &\quad + \mathbf{v}_{i(f,b,u),f,b}^H \mathbf{H}_{i(f,b,u),f} \sum_{\substack{b'=1 \\ b' \neq b}}^B \mathbf{m}_{f,b'} \sum_{u'=1}^{k(f,b')} \sqrt{P_{i(f,b',u'),f,b'}} s_{i(f,b',u'),f,b'} \\ &\quad + \mathbf{v}_{i(f,b,u),f,b}^H \mathbf{w}_{i(f,b,u),f} \end{aligned}. \quad (4)$$

In the paper, we assume that $\mathbf{v}_{i(f,b,u),f,b}$ is calculated based on the minimum mean squared error (MMSE) criteria. The second and third terms of (4) are the inter-beam interference and receiver noise plus inter-cell interference observed at the spatial filtering output, respectively. By normalizing the aggregated power of the inter-beam interference and receiver noise plus inter-cell interference to be one, (4) is rewritten as

$$z_{i(f,b,u),f,b} = \sqrt{g_{i(f,b,u),f,b}} \sum_{u'=1}^{k(f,b)} \sqrt{P_{i(f,b,u'),f,b}} s_{i(f,b,u'),f,b} + q_{i(f,b,u),f,b}, \quad (5)$$

where $q_{i(f,b,u),f,b}$ denotes the sum of the inter-beam interference, receiver noise, and inter-cell interference terms after normalization (thus, $\mathbb{E}[|q_{i(f,b,u),f,b}|^2] = 1$). Term $g_{i(f,b,u),f,b}$ is represented as

$$g_{i(f,b,u),f,b} = \frac{|\mathbf{v}_{i(f,b,u),f,b}^H \mathbf{H}_{i(f,b,u),f} \mathbf{m}_{f,b}|^2}{\left\{ \sum_{b'=1, b' \neq b}^B P_{f,b'} |\mathbf{v}_{i(f,b,u),f,b}^H \mathbf{H}_{i(f,b,u),f} \mathbf{m}_{f,b'}|^2 + \mathbf{v}_{i(f,b,u),f,b}^H \mathbb{E}[\mathbf{w}_{i(f,b,u),f} \mathbf{w}_{i(f,b,u),f}^H] \mathbf{v}_{i(f,b,u),f,b} \right\}}. \quad (6)$$

Thus, among users to which beam b of frequency block f is allocated, the channel after the spatial filtering is a degraded SISO channel, and equivalent normalized channel gain of user $i(f,b,u)$ becomes $g_{i(f,b,u),f,b}$.

We apply the intra-beam SIC to signal $z_{i(f,b,u),f,b}$ in order to remove the inter-user interference within a beam. Similar to the SISO downlink [5], the optimal order of decoding is in the order of the increasing normalized channel gain, $g_{i(f,b,u),f,b}$. Based on this order, any user can correctly decode the signals of other users whose decoding order comes before that user for the purpose of interference cancellation. Thus, user $i(f,b,u)$ can remove the inter-user interference from user $i(f,b,u')$ whose $g_{i(f,b,u'),f,b}$ is lower than $g_{i(f,b,u),f,b}$. As a result, the throughput of user $i(f,b,u)$ at beam b of frequency block f is represented as

$$\begin{aligned} R_{f,b}(i(f,b,u)) &= \\ &= W \log_2 \left(1 + \frac{g_{i(f,b,u),f,b} P_{i(f,b,u),f,b}}{\sum_{\substack{u'=1, g_{i(f,b,u'),f,b} < g_{i(f,b,u),f,b}}}^{k(f,b)} g_{i(f,b,u'),f,b} P_{i(f,b,u'),f,b} + 1} \right), \end{aligned} \quad (7)$$

B. Random Beamforming

Fig. 1 shows the operational flow of random beamforming [10, 11]. First, the base station randomly determines B beamforming vectors without the aid of feedback information from the user terminals. Then, the base station transmits the downlink reference signals before the actual data transmission. The number of reference signals equals the number of beams, B , and the respective reference signals are beamformed by the respective predetermined beamforming vectors. By using the b -th reference signal, the estimate of $\mathbf{H}_{k,f} \mathbf{m}_{f,b}$ is obtained at user terminal k . Using the estimate of $\mathbf{H}_{k,f} \mathbf{m}_{f,b}$ for all B beams, the spatial filtering vector, $\mathbf{v}_{k,f,b}$, is calculated. With $\mathbf{v}_{k,f,b}$ and the estimate of $\mathbf{H}_{k,f} \mathbf{m}_{f,b}$, the equivalent channel gain, $g_{k,f,b}$, is measured using (6). For user k , the signal-to-interference and noise power ratio (SINR) of beam b at frequency block f becomes $\text{SINR}_{k,f,b} = g_{k,f,b} P_b$. User k feeds back $\text{SINR}_{k,f,b}$ to the serving base station. The base station performs multiuser scheduling based on the reported $\text{SINR}_{k,f,b}$ and actual data transmission for the set of the scheduled users is performed using the predetermined beamforming vectors. Since random beamforming only requires the SINR feedback, the feedback overhead is reduced compared to that for closed loop-type beamforming such as the codebook-based or explicit channel feedback-based approaches.

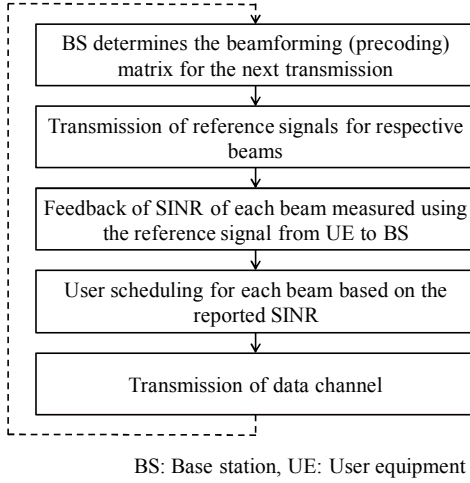


Figure 1. Operational flow of random beamforming.

Although the beamforming vectors are determined independent of the user channel conditions, when the number of candidate users for scheduling is sufficiently large, we can expect that the randomly selected beamforming vector is matched to the channel of some user with high probability. With multiuser scheduling based on the reported SINR, we can select that user effectively. Furthermore, since the beamforming matrix of all cells is determined at the SINR measurement stage, by adequately designing the configuration of the reference signal, the SINR measurement results at the user terminal can take into account the inter-cell interference with beamforming, which is beneficial to achieve distributed inter-cell interference coordination.

III. JOINT POWER ALLOCATION AMONG FREQUENCY BLOCKS AND BEAMS

This paper proposes frequency block-dependent power allocation among beams in conjunction with FFR-like different power allocation among frequency blocks.

Fig. 2 shows the typical FFR method called soft FFR. The overall system transmission bandwidth is divided into two parts: a frequency band with priority given to cell-edge users (edge band hereafter) and that with priority given to cell-interior users (inner band hereafter). The bandwidth for the edge band is assumed to be 1/3 of the overall system transmission bandwidth. Among the three neighboring cells, the edge bands do not overlap as indicated in Fig. 2. The set of all frequency blocks is denoted as $X = \{1, 2, \dots, F\}$. At base station s , the sets of frequency blocks belonging to the edge band and inner band are denoted as $X_{\text{edge}}(s)$ and $X_{\text{inner}}(s)$, respectively. Here, $|X_{\text{edge}}(s) \cap X_{\text{inner}}(s)| = 0$ and $X_{\text{edge}}(s) \cup X_{\text{inner}}(s) = X$. Between neighbor base stations s and s' , $|X_{\text{edge}}(s) \cap X_{\text{edge}}(s')| = 0$. In the paper, the transmission power of a frequency block belonging to the edge band is β -dB higher than that of a frequency block belonging to the inner band.

$$P_{f \in X_{\text{edge}}(s)} = 10^{\beta/10} P_{f \in X_{\text{inner}}(s)}. \quad (8)$$

These settings yield inter-cell interference coordination for the edge band since the increased transmission power density for the edge band and reduced transmission power density for the inner band of neighboring cells results in a better SINR at the edge band.

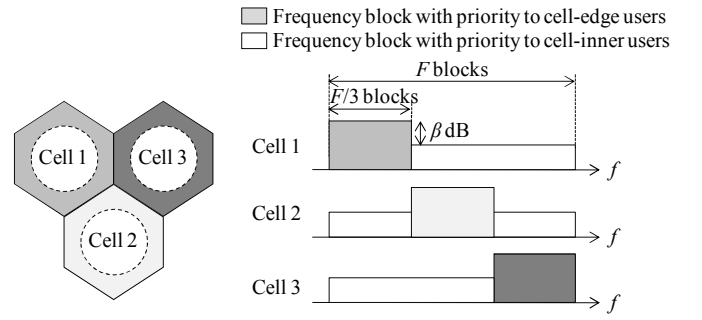


Figure 2. Power allocation among frequency blocks based on FFR.

The proposed method controls the transmission power allocation among beams within a frequency block. Since the FFR assumes that the edge band is mainly used by the cell-edge users and the non-equal transmission power allocation among beams is beneficial for the cell-edge users (opposite happens for inner band), we propose using a different power allocation ratio among beams for the edge and inner bands. Since we assume the B of two beams in the simulation evaluation in Section IV, with power allocation parameter α_{edge} and α_{inner} ($0.5 \leq \alpha_{\text{edge}}, \alpha_{\text{inner}} \leq 1$) for the edge and inner bands, respectively, the transmission power of the respective beams is set as follows.

$$\begin{aligned} P_{f,1} &= \alpha_{\text{edge}} P_f, P_{f,2} = (1 - \alpha_{\text{edge}}) P_f, \quad \text{when } f \in X_{\text{edge}}(s) \\ P_{f,1} &= \alpha_{\text{inner}} P_f, P_{f,2} = (1 - \alpha_{\text{inner}}) P_f, \quad \text{when } f \in X_{\text{inner}}(s) \end{aligned} \quad (9)$$

The α_{edge} or α_{inner} of 0.5 corresponds to equal power allocation between the two beams. As will be described in Section IV, by setting α_{edge} higher than α_{inner} , we can increase the cell-edge user throughput at a small sacrifice of the average user throughput.

IV. SIMULATION RESULTS

Here we evaluate the distribution of the user throughput in a multi-cell downlink. Table I gives the simulation parameters.

A 19-cell model with a hexagonal grid is used. The inter-site distance is 500 m. The number of users per cell is 30. The locations of the user terminals in each cell are randomly assigned with a uniform distribution. The values for W and F are set to 180 kHz [1] and 24, respectively (overall transmission bandwidth is 4.32 MHz). The transmission power at the base station is 40 dBm. For FFR, eight frequency blocks per cell are used for the edge band. The set of randomly generated orthogonal vectors are used as a beamforming matrix. The values of M , B , and N are set to two. We take into account the distance-dependent path loss with the decay factor of 3.76, lognormal shadowing with the standard deviation of 8 dB and 0.5-correlation among sites, 6-path Rayleigh fading with the rms delay spread of 1 μ s, and the maximum Doppler frequency of 55.5 Hz. The receiver noise density of the user terminal is -169 dBm/Hz.

TABLE I. SIMULATION PARAMETERS

Cell layout		Hexagonal 19-cell model without sectorization
Frequency reuse		Universal frequency reuse
Inter-site distance		0.5 km
Overall transmission bandwidth		4.32 MHz
Resource block bandwidth		180 kHz
Number of resource blocks		24
Number of UEs per cell		30
BS transmitter antenna	Number of antennas	$M = 1, 2$
	Antenna gain	14 dBi
	Number of beams	$B = M$
UE receiver antenna	Number of antennas	$N = 2$
	Antenna gain	0 dBi
Beamforming matrix		Random unitary matrix (orthonormal vectors)
Receiver linear filtering		MMSE-based
Maximum transmission power		40 dBm
Distance-dependent path loss		$128.1 + 37.6 \log_{10}(r)$ dB, r : kilometers
Log-normal shadowing		$\delta = 8$ dB, Correlation among cells = 0.5
Instantaneous fading		Six-path Rayleigh, rms delay spread = 1 μ s, $f_D = 55.5$ Hz
Receiver noise density		-169 dBm/Hz
Scheduling interval		1 ms
Throughput calculation		Based on Shannon formula (Max. 6 b/s/Hz)
Averaging interval of user throughput		100 ms (1-ms packet length)

The radio resource (beam of each frequency block and power) allocation to users is updated every 1 ms. We assume proportional fair (PF)-based resource (power and frequency) allocation [9] to achieve a good tradeoff between them by maximizing the product of the average user throughput among users within a cell. The maximum number of non-orthogonally multiplexed users per frequency block is set to 2. The user throughput averaged over 100 ms is measured. The user throughput is calculated based on the Shannon formula with the maximum limit of 6 b/s/Hz (corresponding to 64QAM). In the following, we simply denote the average user throughput of 100 ms as the user throughput to avoid confusion with the average of the throughput among users within a cell. In the following, the average user throughput, R_{avg} , and the cell-edge user throughput, R_{edge} , defined as the user throughput value at the cumulative probability of 5% [1, 2] are examined.

Figs. 3 and 4 show R_{avg} and R_{edge} as a function of β , respectively. Four cases with $(\alpha_{\text{edge}}, \alpha_{\text{inner}})$ of (0.5, 0.5), (0.9, 0.9), (0.5, 0.9), and (0.9, 0.5) are tested. Overall, as β is increased, R_{avg} is decreased while R_{edge} is increased. This is because since an increase in β equivalently corresponds to the decrease in the frequency reuse factor, the system-level efficiency measured by R_{avg} is degraded compared to the case with the β of 0 dB which corresponds to universal frequency reuse. However, since the SINR at the edge band is increased due to the increased signal power and decreased inter-cell interference as β is increased, R_{edge} is increased. When we control the α_{edge} and α_{inner} other than both 0.5, R_{avg} is further decreased while R_{edge} is further increased. We see that the

improvement in R_{edge} is limited when $(\alpha_{\text{edge}}, \alpha_{\text{inner}})$ is (0.5, 0.9), thus α_{edge} is smaller than α_{inner} . With the $(\alpha_{\text{edge}}, \alpha_{\text{inner}})$ of (0.9, 0.5), thus when α_{edge} is larger than α_{inner} , significant enhancement of R_{edge} is achieved while minimizing the degradation in R_{avg} . This tendency is especially significant when β is large such as beyond 15 dB. In such a case, the use of $(\alpha_{\text{edge}}, \alpha_{\text{inner}})$ of (0.9, 0.5) achieves almost the same R_{edge} as that with $\alpha_{\text{edge}} = \alpha_{\text{inner}} = 0.9$, while R_{avg} is much higher. This is because the higher α_{edge} setting is appropriate for the cell-edge users and in FFR-like power allocation among frequency blocks, the edge band is effectively used by the cell-edge users. The lower α_{inner} setting is appropriate for the cell-interior users, and in FFR-like power allocation, the inner band is effectively used by the cell-interior users. Therefore, severe degradation in R_{avg} is avoided. From these results, we see that the FFR-like power allocation among frequency blocks and frequency block-dependent power allocation among beams achieves a synergistic effect for improving the tradeoff between R_{avg} and R_{edge} .

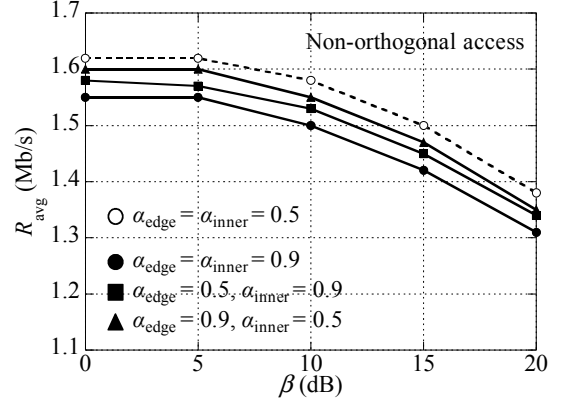


Figure 3. R_{avg} as a function of β .

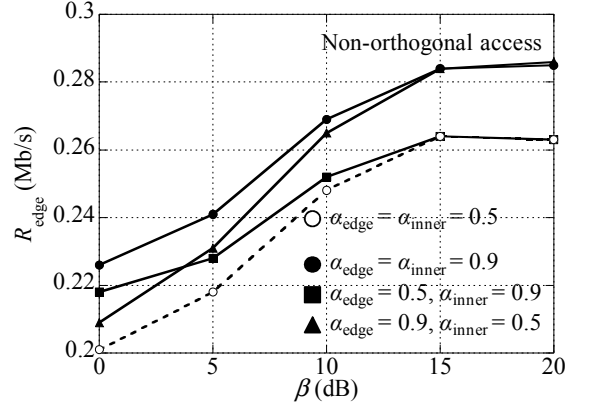


Figure 4. R_{edge} as a function of β .

Figs. 5 and 6 show R_{avg} and R_{edge} as a function of α_{edge} , respectively, assuming that α_{inner} is fixed to 0.5. The β value is parameterized. As α_{edge} is increased, R_{avg} decreases while R_{edge} increases. This is because equal power allocation among multiple beams enhances the average user throughput within a cell due to the effective use of spatial multiplexing. The throughput of users at the cell edge is improved by non-equal transmission power allocation among beams since the inter-beam interference is decreased and the received signal power is increased from the viewpoint of the main beam to which most of the transmission power is allocated. However, it should be noted that when β is high, the increasing ratio of R_{edge} as α_{edge} is

increased is higher than the decreasing ratio of R_{avg} . Therefore, for the effective enhancement of R_{edge} , increasing α_{edge} in addition to the use of a high β value is effective.

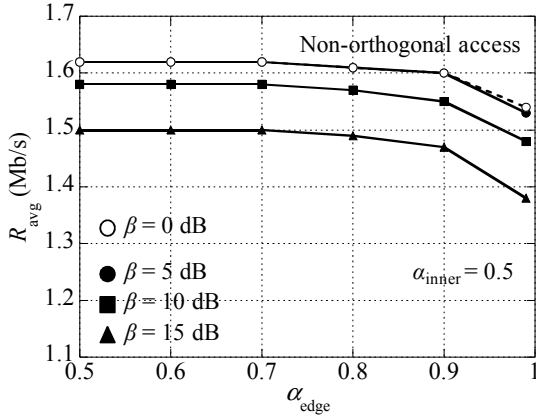


Figure 5. R_{avg} as a function of α_{edge} (α_{inner} is fixed to 0.5).

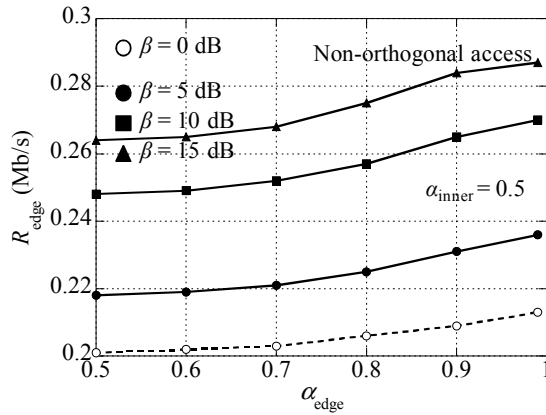


Figure 6. R_{edge} as a function of α_{edge} (α_{inner} is fixed to 0.5).

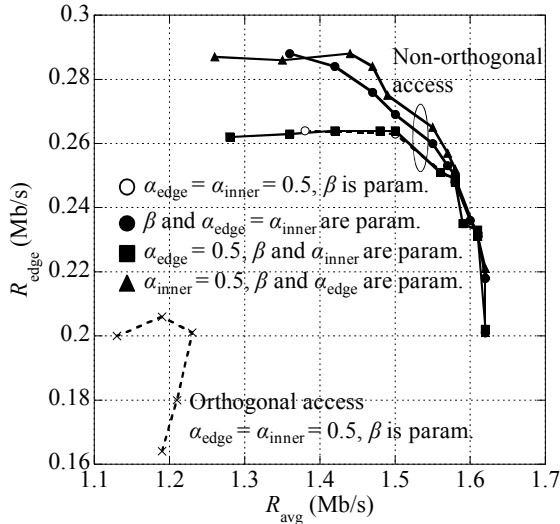


Figure 7. R_{edge} as a function of R_{avg} .

Fig. 7 shows R_{edge} as a function of R_{avg} . Four cases are examined: (a) (α_{edge} , α_{inner}) is fixed to (0.5, 0.5) and β is parameterized for changing the relation between R_{edge} and R_{avg} ;

(b) both $\alpha_{\text{edge}} = \alpha_{\text{inner}}$ and β are parameterized; (c) α_{edge} is fixed to 0.5, and α_{inner} and β are parameterized; (d) α_{inner} is fixed to 0.5, and α_{edge} and β are parameterized. For comparison the performance of orthogonal access is also shown. As is expected, case (d) yields the largest $R_{\text{edge}} - R_{\text{avg}}$ region. Significant R_{edge} and R_{avg} enhancements by using the proposed non-orthogonal access with intra-beam SIC compared to the orthogonal access are also confirmed.

V. CONCLUSION

Aiming at further enhancement of the system efficiency and cell-edge user experience of our previously proposed non-orthogonal access with intra-beam superposition coding and SIC along with random beamforming, a joint transmission power allocation control method among frequency blocks and beams was proposed. By equally allocating transmission power among multiple beams, the average user throughput within a cell can be enhanced due to the effective use of spatial multiplexing. The throughput of users at the cell edge may be improved by non-equal transmission power allocation among beams since the inter-beam interference is decreased and the received signal power is increased from the viewpoint of the main beam to which most of the transmission power is allocated. The FFR-like power allocation among frequency blocks achieves the inter-cell interference coordination effect. This paper showed that by coordinating the inter-beam power allocation and inter-frequency block power allocation, the cell-edge user throughput is significantly increased at the cost of a small reduction in the cell-average user throughput.

REFERENCES

- [1] 3GPP TS36.300, Evolved Universal Terrestrial Radio Access (E-UTRA) and Evolved Universal Terrestrial Radio Access Network (E-UTRAN); Overall description.
- [2] 3GPP TR36.913 (V8.0.0), "3GPP; TSG RAN; Requirements for further advancements for E-UTRA (LTE-Advanced)," June 2008.
- [3] 3GPP TR36.814 (V9.0.0), "Further advancements for E-UTRA physical layer aspects," Mar. 2010.
- [4] G. Caire and S. Shamai (Shitz), "On the achievable throughput of a multi-antenna Gaussian broadcast channel," IEEE Trans. Inf. Theory, vol. 49, no. 7, pp. 1692-1706, July 2003.
- [5] P. Viswanath and D. N. C. Tse, "Sum capacity of the vector Gaussian broadcast channel and uplink-downlink duality," IEEE Trans. Inf. Theory, vol. 49, no. 8, pp. 1912-1921, Aug. 2003.
- [6] S. Vishwanath, N. Jindal, and A. Goldsmith, "Duality, achievable rates and sum rate capacity of Gaussian MIMO broadcast channel," IEEE Trans. Inf. Theory, vol. 49, no. 10, pp. 2658-2668, Oct. 2003.
- [7] H. Weingarten, Y. Steinberg, and S. Shamai (Shitz), "The capacity region of Gaussian MIMO broadcast channel," in Proc. IEEE ISIT2004, Chicago, IL, Jun./Jul. 2004.
- [8] N. Otao, Y. Kishiyama, and K. Higuchi, "Performance of non-orthogonal access with SIC in cellular downlink using proportional fair-based resource allocation," in Proc. IEEE ISWCS2012, Paris, France, Aug. 2012.
- [9] K. Higuchi and Y. Kishiyama, "Non-orthogonal access with random beamforming and intra-beam SIC for cellular MIMO downlink," in Proc. IEEE VTC2013-Fall, Las Vegas, U.S.A., 2-5 Sep. 2013.
- [10] P. Viswanath, D. N. C. Tse, and R. Laroia, "Opportunistic beamforming using dumb antennas," IEEE Trans. Inf. Theory, vol. 48, no. 6, pp. 1277-1294, June 2002.
- [11] M. Sharif and B. Hassibi, "On the capacity of MIMO broadcast channels with partial side information," IEEE Trans. Inf. Theory, vol. 51, no. 2, pp. 506-522, Feb. 2005.
- [12] S. E. Elayoubi, O. B. Haddada, and B. Foudrestie, "Performance evaluation of frequency planning schemes in OFDMA-based networks," IEEE Trans. Wireless Commun., vol. 7, no. 5, pp. 1623-1633, May 2008.
- [13] R. Giuliano, C. Monti, and P. Loreti, "WIMAX fractional frequency reuse for rural environments," IEEE Wireless Commun. Mag., vol. 15, no. 3, pp. 60-65, Jun. 2008.